Understanding Bottom Production*

N. Kidonakis[a,b], E. Laenen[c], S. Moch[d] and R. Vogt[e,f]

[a]Department of Physics and Astronomy, University of Rochester, Rochester, NY USA

[b]Department of Physics, Southern Methodist University, Dallas, TX USA

[c]NIKHEF Theory Group, 1009 DB Amsterdam, The Netherlands

[d]Institut für Theoretische Teilchenphysik, Universität Karlsruhe, Germany

[e]Lawrence Berkeley National Laboratory, Berkeley, CA USA

[f]Physics Department, University of California, Davis, CA USA

We describe calculations of $b\overline{b}$ production to next-to-next-to-leading order (NNLO) and next-to-next-to-leading logarithm (NNLL) near threshold in pp interactions. Our calculations are in good agreement with the $b\overline{b}$ total cross section measured by HERA-B.

Factorization assumes it is possible to separate QCD cross sections into universal, non-perturbative parton densities and a perturbatively calculable hard scattering function, the partonic cross section. However, some remnants of long-distance dynamics in the hard scattering function can dominate corrections at higher orders near production threshold. These Sudakov corrections have the form of distributions singular at partonic threshold. Threshold resummation techniques organize the singular distributions to all orders, extending the reach of QCD into near threshold production. The singular functions organized by resummmation are the plus distributions, $[\ln^l x/x]_+$, where x denotes the 'distance' from partonic threshold.

The first attempts to resum the heavy quark cross section were at leading logarithm (LL) and exploited the fact that to LL, the Sudakov corrections to the heavy quark cross section were identical to those obtained for Drell-Yan production [1–3]. This early resummation calculation, like some of the later results that followed, used an empirical cutoff to keep the strong coupling constant from blowing up. Resummation beyond LL cannot make use of this universality because the color structure of each partonic process must be treated separately [4]. The NLL $Q\overline{Q}$ terms were first resummed in Ref. [5] for a simplified case and later fully solved for the $q\overline{q}$ channel [6]. The exponents in the gg channel were calculationally unwieldly, requiring large cutoffs even for $t\overline{t}$ production where the resummation should work best. However, one advantage of the resummed cross

*This work was supported in part by the Director, Office of Energy Research, Division of Nuclear Physics of the Office of High Energy and Nuclear Physics of the U. S. Department of Energy under Contract No. DE-AC03-76SF0098.

section is that when it is expanded in powers of α_s, it provides estimates of unknown finite-order corrections without resorting to a cutoff or other prescriptions. We have calculated the double-differential heavy quark hadroproduction cross sections up to next-to-next-to-leading order (NNLO), $\mathcal{O}(\alpha_s^4)$, and next-to-next-to-leading logarithm (NNLL), *i.e.* keeping powers of the singular functions as low as $l = 2i-1$ at order $\mathcal{O}(\alpha_s^{i+3})$ where $i = 0, 1, \ldots$ [7,8]. Since resummation is based on expansion of the LO cross section, we only discuss $Q\overline{Q}$ production in the $ij = q\overline{q}$ and gg channels since qg scattering first appears at NLO.

In our calculations, the distance from partonic threshold in the singular functions depends on how the cross section is calculated, either by integrating away the momentum of the unobserved heavy quark or antiquark and determining the one-particle inclusive (1PI) cross section for the detected quark, or by treating the Q and $\overline{Q}$ as a pair in the integration, pair invariant mass (PIM) kinematics. In 1PI kinematics,

$$p(P_1) + p(P_2) \longrightarrow Q(p_1) + X(p_X)\,, \tag{1}$$

where X denotes any hadronic final state containing the heavy antiquark and $Q(p_1)$ is the identified heavy quark. The reaction in Eq. (1) is dominated by the partonic reaction

$$i(k_1) + j(k_2) \quad \longrightarrow \quad Q(p_1) + X[\overline{Q}](p_2')\,. \tag{2}$$

At LO or if $X[\overline{Q}](p_2') \equiv \overline{Q}(\overline{p}_2)$, the reaction is at partonic threshold with $\overline{Q}$ momentum $\overline{p}_2$. At threshold the heavy quarks are not necessarily produced at rest but with equal and opposite momentum. The partonic Mandelstam invariants are

$$s = (k_1 + k_2)^2\,, \quad t_1 = (k_2 - p_1)^2 - m^2\,, \quad u = (k_1 - p_1)^2 - m^2\,, \quad s_4 = s + t_1 + u_1 \tag{3}$$

where the last, $s_4 = (p_2')^2 - m^2$, is the inelasticity of the partonic reaction. At threshold, $s_4 = 0$. Thus the distance from threshold in 1PI kinematics is $x = s_4/m^2$. In 1PI kinematics, the cross sections are functions of t_1 and u_1. In PIM kinematics the pair is treated as a unit so that, on the partonic level, we have

$$i(k_1) + j(k_2) \quad \longrightarrow \quad Q\overline{Q}(p') + X(k')\,. \tag{4}$$

The square of the heavy quark pair mass is $p'^2 = M^2$. At partonic threshold, $X(k') = 0$, the three Mandelstam invariants are

$$s = M^2\,, \quad t_1 = -\frac{M^2}{2}(1 - \beta_M\,\cos\theta)\,, \quad u_1 = -\frac{M^2}{2}(1 + \beta_M\,\cos\theta) \tag{5}$$

where $\beta_M = \sqrt{1 - 4m^2/M^2}$ and θ is the scattering angle in the parton center of mass frame. Now the distance from threshold is $x = 1 - M^2/s \equiv 1 - z$ where $z = 1$ at threshold. In PIM kinematics the cross sections are functions of M^2 and $\cos\theta$.

The resummation is done in moment space by making a Laplace transformation with respect to x, the distance from threshold. Then the singular functions become linear combinations of $\ln^k \tilde{N}$ with $k \leq l+1$ and $\tilde{N} = Ne^{\gamma_E}$ where γ_E is the Euler constant. The 1PI resummed double differential partonic cross section in moment space is

$$s^2 \frac{d^2\sigma_{ij}^{\rm res}(\tilde{N})}{dt_1\,du_1} = {\rm Tr}\Bigg\{ H_{ij} \bar{\rm P} \exp\left[\int_m^{m/\tilde{N}} \frac{d\mu'}{\mu'} (\Gamma_S^{ij}\,(\alpha_s(\mu')))^\dagger\right] \tilde{S}_{ij} {\rm P} \exp\left[\int_m^{m/\tilde{N}} \frac{d\mu'}{\mu'} \Gamma_S^{ij}\,(\alpha_s(\mu'))\right]\Bigg\} \tag{6}$$

$$\times \exp\left(\tilde{E}_i(\tilde{N}_u, \mu, \mu_R)\right)\, \exp\left(\tilde{E}_j(\tilde{N}_t, \mu, \mu_R)\right)\, \exp\left\{2\int_{\mu_R}^{m} \frac{d\mu'}{\mu'} \left(\gamma_i\,(\alpha_s(\mu')) + \gamma_j\,(\alpha_s(\mu'))\right)\right\}.$$

To find the PIM result, transform t_1 and u_1 to M^2 and $\cos\theta$ using Eq. (5). $(\overline{\mathrm{P}})$ P refer to (anti-)path ordering in scale μ'. The cross section depends on the 'hard', H_{ij}, and 'soft', $\tilde{S}_{ij}$, hermitian matrices. The 'hard' part contains no singular functions. The 'soft' component contains the singular functions and, from its renormalization group equation, the soft anomalous dimension matrix Γ_S^{ij}, 2 dimensional for $q\overline{q}$ and 3 for gg, can be derived. The universal Sudakov factors, the same in 1PI and PIM, are in the exponents $\tilde{E}_i$, expanded as

$$\exp(\tilde{E}_i(\tilde{N}_u,\mu,m)) \simeq 1 + \frac{\alpha_s}{\pi}\left(\sum_{k=0}^{2} C_k^{i,(1)} \ln^k(\tilde{N}_u)\right) + \left(\frac{\alpha_s}{\pi}\right)^2 \left(\sum_{k=0}^{4} C_k^{i,(2)} \ln^k(\tilde{N}_u)\right) + \ldots \, . \quad (7)$$

The coefficients $C_k^{i,(n)}$, as well as the detailed derivation of the resummed and finite-order cross sections, can be found in Ref. [7]. The momentum space cross sections to NNLO-NNLL are obtained by gathering terms at $\mathcal{O}(\alpha_s^3)$ and $\mathcal{O}(\alpha_s^4)$, inverting the Laplace transformation and matching the $\tilde{N}$-independent terms in H_{ij} and $\tilde{S}_{ij}$ to exact $\mathcal{O}(\alpha_s^3)$ results.

We have studied the partonic and hadronic total cross sections of $t\overline{t}$ and $b\overline{b}$ production. Any difference in the integrated cross sections due to kinematics choice arises from the ambiguity of the estimates. At leading order, no additional soft partons are produced and the threshold condition is exact. Therefore, there is no difference between the total cross sections in the two kinematic schemes. However, beyond LO and threshold there is a difference. To simplify the argument, the total partonic cross section may be expressed in terms of dimensionless scaling functions $f_{ij}^{(k,l)}$ that depend only on $\eta = s/4m^2 - 1$ [7],

$$\sigma_{ij}(s,m^2,\mu^2) = \frac{\alpha_s^2(\mu)}{m^2} \sum_{k=0}^{\infty} \, (4\pi\alpha_s(\mu))^k \sum_{l=0}^{k} \, f_{ij}^{(k,l)}(\eta) \, \ln^l\left(\frac{\mu^2}{m^2}\right) . \quad (8)$$

We have constructed LL, NLL, and NNLL approximations to $f_{ij}^{(k,l)}$ in the $q\overline{q}$ and gg channels for $k \leq 2$, $l \leq k$. Exact results are known for $k=1$ and can be derived using renormalization group methods for $k=2$, $l=1,2$. Thus the best NNLO estimate of the cross section includes the exact scaling functions and the NNLL estimate of $f_{ij}^{(2,0)}$. On the left-hand side of Fig. 1, we compare $f_{q\overline{q}}^{(2,0)}$ and $f_{gg}^{(2,0)}$, the only approximate scaling function, in 1PI and PIM. The results are quite similar at small η but begin to differ for $\eta \geq 0.1$, especially in the gg channel. If the parton flux is maximized for $\eta < 1$, as for the HERA-B energy, $\sqrt{S} = 41.6$ GeV, the reaction is close enough to threshold for the results to be reliable. Unfortunately at RHIC, the flux peaks at $\eta \approx 1$, making predictions at RHIC from the threshold approximation alone unreliable. The gg channel dominates $b\overline{b}$ production in pp interactions. An inspection of the scaling functions shows that the results could differ substantially between the two kinematics.

The total hadronic cross section is obtained by convoluting the total partonic cross section with the parton densities f_i^p evaluated at momentum fraction x and scale μ,

$$\sigma_{pp}(S,m^2) = \sum_{i,j=q,\overline{q},g} \int_{4m^2/S}^{1} d\tau \int_{\tau}^{1} \frac{dx_1}{x_1} f_i^p(x_1,\mu^2) f_j^p\left(\frac{\tau}{x_1},\mu^2\right) \sigma_{ij}(\tau S,m^2,\mu^2) \, . \quad (9)$$

If the peak of the convolution of the parton densities is at $\eta < 1$, the approximation should hold. On the right-hand side of Fig. 1 we compare the 1PI and PIM results with

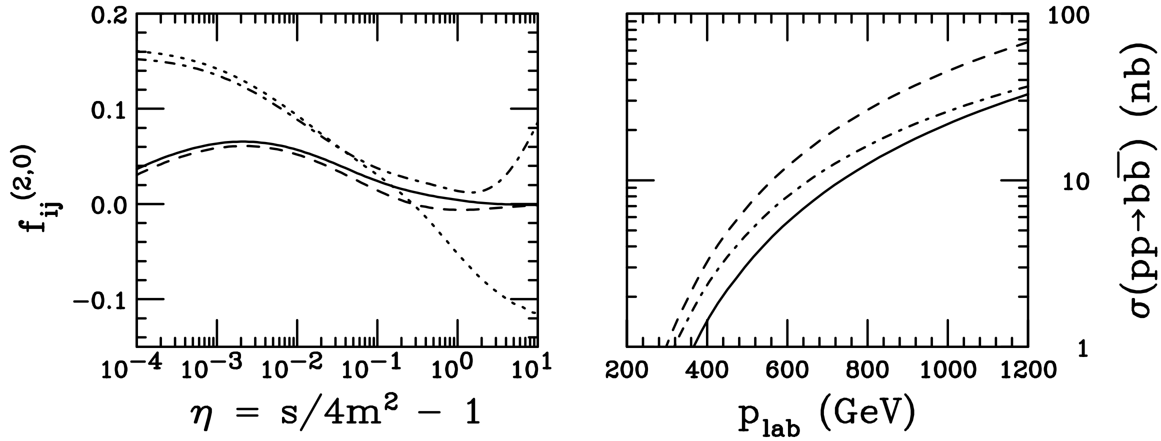

Figure 1. The left-hand side shows the η-dependence of the NNLL scaling functions. We show $f_{q\bar{q}}^{(2,0)}(\eta)$ in 1PI (solid) and PIM (dashed) kinematics and $f_{gg}^{(2,0)}(\eta)$ in 1PI (dot-dashed) and PIM (dotted) kinematics. The right-hand side compares the total $b\bar{b}$ cross sections at fixed target energies calculated with CTEQ5M and $\mu = m = 4.75$ GeV. The exact NLO result is shown in the solid curve while the NNLO-NNLL results for 1PI and PIM kinematics are given by the dashed and dot-dashed curves respectively.

the exact NLO results, all calculated with the CTEQ5M parton densities [9] and $\mu = m$. The NNLO-NNLL corrections are substantial. The average of the NNLO-NNLL 1PI and PIM cross sections,

$$\sigma_{b\bar{b}}(41.6\,\mathrm{GeV}) = 30 \pm 8 \pm 10\,\mathrm{nb}\ , \tag{10}$$

is in good agreement with the $b\bar{b}$ total cross section measured by HERA-B [10]. The first uncertainty is due to the kinematics choice, the second to the scale dependence. The uncertainties in scale and kinematics choice are essentially equivalent.

REFERENCES

1. E. Laenen, J. Smith, and W.L. van Neerven, Nucl. Phys. **B369** (1992) 543.
2. N. Kidonakis and J. Smith, Phys. Rev. **D51** (1995) 6092; Mod. Phys. Lett. **A11** (1996) 587.
3. J. Smith and R. Vogt, Z. Phys. **C75** (1997) 271.
4. N. Kidonakis and G. Sterman, Phys. Lett. **B387** (1996) 867; Nucl. Phys. **B505** (1997) 321.
5. N. Kidonakis, J. Smith, and R. Vogt, Phys. Rev. **D56** (1997) 1553.
6. N. Kidonakis and R. Vogt, Phys. Rev. **D59** (1999) 074014.
7. N. Kidonakis, E. Laenen, S. Moch, and R. Vogt, Phys. Rev. **D64** (2001) 114001.
8. N. Kidonakis, Phys. Rev. **D64** (2001) 014009.
9. H.L. Lai *et al.*, Eur. Phys. J. **C12** (2000) 375.
10. I. Abt *et al.* (HERA-B Collab.), hep-ex/0205106; A. Zoccoli, these proceedings.